

Variational Bayesian Image Reconstruction with an Uncertainty Model for Measurement Localization

Filip Sroubek, Jindřich Soukup and Barbara Zitová

Institute of Information Theory and Automation, Czech Academy of Sciences

Pod Vodárenskou věží 4, 182 08 Prague 8, Czech Republic

Email: sroubekf@utia.cas.cz

Abstract—We propose a general data acquisition model with volatile random displacement of measured samples. Discrepancies between recorded and true positions of the original data is due to the nature of measured data or the acquisition device itself. A reconstruction method based on the Variational Bayesian inference is proposed, which estimates the original data from samples acquired with the acquisition model, and its relation to Jensen’s inequality is discussed. A model variant of 2D image reconstruction is analyzed in detail. Further, we outline a relation between the proposed method and the classic deconvolution problem, and illustrate superiority of the Variational Bayesian approach in the case of small number of samples.

I. INTRODUCTION

A data acquisition process is influenced by many imperfections related to the measuring device and the setup itself. The resulting data exhibit degradation of various forms such as blur, noise, low contrast, incomplete measurements or spatial deformations. In this paper we address the degradation caused by random spatial displacement of measured samples. Due to the nature of studied objects or the measuring device, the acquired data can have erroneous spatial correspondences between recorded and true positions of individual object parts. Such random localization discrepancies negatively influence further data analysis if they are not taken into consideration.

We distinguish two types of position discrepancies: displacement induced by the measured object itself, and displacement caused by the acquisition sensor. The first type of position uncertainty is common in devices that record low-energy radiation (such as single photons) with strong scattering phenomena. Examples are positron emission tomography (PET) or some types of fluorescence microscopy, such as photo-activated localization microscopy (PALM) [1]. A scattered incident radiation coming from a scanned object activates different sensor segments, which results in the disrupted spatial relationship of the object and its captured representation. The resulting dataset then exhibits jitters as shown, e.g., in Fig. 1(b).

An example of the second type is free-hand 3D ultrasound (US) imaging [2]. A sequence of 2D slice images acquired by a hand-held ultrasound probe is used to generate a 3D volume. One option is to estimate the geometrical relationship of slices from the data itself or, which is more accurate, to use a tracking system to record the probe position in time. In both cases uncertainty in estimating the probe position causes blur artifacts in 3D volume reconstruction and should be

thus considered in the model [3]. Another example, e.g. from computer vision, is the structure-from-motion problem [4]. An inaccurate estimation of camera position implies artifacts in 3D object reconstruction. In compressed sensing the problem of grid mismatch [5] is also related to our formulation.

In this work, we formalize an acquisition model with uncertainty that describes random displacement of measured samples, and propose a reconstruction method based on the Variational Bayesian (VB) inference, which inverts the acquisition process and estimates latent data. We compare with a reconstruction method based on Jensen’s inequality and provide detailed analysis of 2D image reconstruction, which is one variant of the acquisition model. In this case the uncertainty is in pixel localization, i.e., each pixel is randomly displaced. If a large number of measurements is acquired, we show that the proposed method converges to the classic deconvolution problem. The challenging part is when the number of measurements is small, which is the case when the Variational Bayesian approach proves to be advantageous.

The paper is organized as follows. Sec. II introduces the acquisition model with the uncertainty in measurement localization and defines necessary probability density functions, such as likelihood and priors. Sec. III presents a solution to the reconstruction problem using Jensen’s inequality and Variational Bayes. In Sec. IV, we apply the proposed solution to the 2D image reconstruction and derive corresponding equations. Experimental Sec. V compares performance using both subjective (visual perception) and objective measures. Sec. VI concludes the paper.

II. MODEL WITH UNCERTAINTY

We assume the following acquisition model. Let u denotes latent data of any dimension (typically 2D or 3D). Suppose we have a device that measures samples of u at some location i but the localization of samples is imprecise. The device can repeat measurements at the presumed location i and for each k -th measurement acquires a sample $g_k(i)$ corrupted by an additive noise n_k . Since the location randomly varies, the true location during the k -th measurement is $i + t_k$, where t_k is a random variable of some known distribution. Let $S(i, t_k)$ denote a linear sampling operator modeling the k -th measuring process at the location i , then the acquisition model takes the form

$$g_k(i) = S(i, t_k)u + n_k.$$

For example, let us consider the 2D image reconstruction from pixel samples with uncertainty in the pixel position. In this case, u represents a 2D image and $g_k(i)$ is a single pixel measured at the 2D position i . The sampling operator $S(i, t_k)$ returns a value at the $(i + t_k)$ -th position, i.e. $S(i, t_k)u = u(i + t_k)$. In the case of free-hand US 3D reconstruction, the same model holds with variables residing in higher dimensions. Latent data u represents a 3D volume, $g_k(i)$ is a 2D image acquired with the US device, and i is a vector of six parameters (6 DOF) defining the US probe position measured by a tracking system. The sampling operator $S(i, t_k)$ extracts from u an image in a 2D plane defined by parameters $(i + t_k)$. Various other measuring scenarios can be represented by this model. The following derivation of VB reconstruction is general and independent of the chosen scenario, but we will demonstrate its application on 2D image reconstruction (in Sec. IV).

The total number of measurements is K and we will consider a single location i . Simplifying the notation by omitting i , the acquisition model becomes a set of K equations

$$g_k = S(t_k)u + n_k, \quad k = 1, \dots, K. \quad (1)$$

Let $\bar{g} = \frac{1}{K} \sum_k g_k$ denote the mean observed sample. The Bayesian paradigm starts with defining the posterior distribution

$$p(u, t|\bar{g}) \propto p(\bar{g}|u, t)p(u)p(t) \quad (2)$$

assuming that u and t are independent. We are interested in u and the random displacement t is a nuisance variable. First, we have to find expressions for the likelihood and priors. Let $t = [t_1, \dots, t_k]$ and n_k be white Gaussian noise with distribution $\mathcal{N}(n_k|0, \gamma^{-1})$, then the likelihood of \bar{g} is

$$p(\bar{g}|u, t) \propto \exp \left\{ -\frac{K\gamma}{2} \left\| \left[\frac{1}{K} \sum_k S(t_k) \right] u - \bar{g} \right\|^2 \right\}. \quad (3)$$

We can assume that measurements are independent and thus priors of random displacements $p(t_k)$ are independent. The distribution of $p(t_k)$ is fully defined by the measuring setup and must be known in advance. As will be clear later, the derivation is independent of the used distribution, we can use any type. e.g. $\mathcal{N}(t_k|0, \alpha^{-1})$ gives

$$p(t) = \prod_k p(t_k) \propto \exp \left\{ -\frac{\alpha}{2} \sum_k \|t_k\|^2 \right\} \quad (4)$$

For simplicity, we consider a normal distribution of image derivatives as an image prior $p(u)$,

$$p(u) \propto \exp \left\{ -\frac{\beta}{2} \|Du\|^2 \right\}, \quad (5)$$

where D is a differential operator. For natural images it would be more appropriate to use heavy-tailed distributions (Laplacian, Gaussian mixtures, Student's t) instead. The derivation would be still tractable, following a guideline outlined in [6], but the final equations become slightly more complicated.

Our ultimate goal is to estimate u with the highest posterior probability. The displacement t is a nuisance variable and so

our inference approach is to marginalize over t to obtain a conditional distribution

$$p(u|\bar{g}) \propto \int p(\bar{g}|u, t)p(u)p(t)dt \quad (6)$$

and then estimate u by minimizing $-\log p(u|\bar{g})$. The displacement t appears non-trivially in $S(t_k)$ and thus solving the integral analytically is intractable.

III. APPROXIMATION AND INFERENCE

To perform inference in our model, one option is to linearize S using a Taylor series, as done e.g. in [3], and solve the integral in (6). Another option, which we will investigate in more detail later, is to calculate a lower bound on $\log p(u|\bar{g})$ using Jensen's inequality:

$$-\log p(u|\bar{g}) \leq \int \frac{K\gamma}{2} \left\| \left[\sum_k \frac{S(t_k)}{K} \right] u - \bar{g} \right\|^2 p(t)dt + \frac{\beta}{2} \|Du\|^2 + \text{const.} \quad (7)$$

Integration is still generally intractable, but for example in the case of 2D image reconstruction as shown in the next section it is solvable and leads to relatively simple equations. However, Jensen's inequality is a lower bound on the marginalized probability, which causes sub-optimal performance in the case of small number of measurement K .

If we want a method that performs better for small K , ideally $K = 1$, we need a better approximation of the posterior probability $p(u, t|\bar{g})$. A natural choice is to apply the VB framework [7] and approximate the posterior by a factorized probability $q(u)q(t)$, where $q(t) = \prod_k q(t_k)$. The individual factors are then calculated iteratively:

$$-\log q(u) = -\mathbb{E}_{q(t)}[\log p(u, t|\bar{g})] = \int \frac{K\gamma}{2} \left\| \left[\sum_k \frac{S(t_k)}{K} \right] u - \bar{g} \right\|^2 q(t)dt + \frac{\beta}{2} \|Du\|^2 + \text{const.} \quad (8)$$

and

$$-\log q(t_k) = -\mathbb{E}_{q(u), q(t_{l \neq k})}[\log p(u, t|\bar{g})] = \frac{\gamma}{2K} \|S(t_k)\bar{u} - g_k\|^2 + \frac{\alpha}{2} \|t_k\|^2 + \text{const.} \quad (9)$$

where by $q(t_{l \neq k})$ we mean all factors $q(t_1), \dots, q(t_K)$ except $q(t_k)$. A few remarks should be made here. The calculation of $q(u)$ in (8) is equivalent to Jensen's inequality (7) except marginalization is not over the prior $p(t)$ but over $q(t)$ estimated in the previous iteration. To avoid the calculation of $q(u)$ covariance, we constrain $q(u)$ to a delta distribution $\delta(u - \bar{u})$, where $\bar{u} = \mathbb{E}_{q(u)}[u] = \arg \min_u -\log q(u)$. The last equality of the factor $q(t_k)$ in (9) was then derived by ignoring the covariance of u and assuming that

$$\mathbb{E}_{q(t_{l \neq k})} \left[K\bar{g} - \sum_{l \neq k} S_l \bar{u} \right] = g_k, \quad (10)$$

which holds only if \bar{u} and \bar{t} are equal to the correct values. At initial iterations this is definitely not true and thus (10) is a simplification. Nevertheless, we adopt this formula to make the calculation of $q(t)$ tractable.

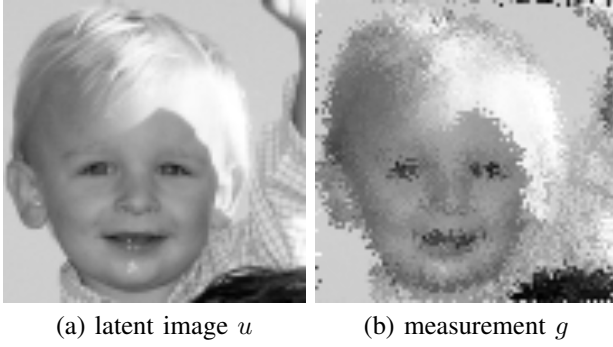


Fig. 1. 2D image reconstruction example: (a) original latent image, (b) one degraded measurement.

IV. 2D IMAGE RECONSTRUCTION

To get a better understanding of the proposed acquisition model and its solution, we derive discrete equations for the case of the 2D image reconstruction. As mentioned earlier, in this case $g_k(i)$ is a measurement of a single pixel of u at the position $(i + t_k)$. Typical prior distributions $p(t_k)$ give lower probabilities to larger displacements and can be thus assumed to have finite support. Then t_k is limited and if discretized it takes a state from a finite list of integer values. We rewrite the acquisition model (1) to consider all pixels simultaneously:

$$\mathbf{g}_k = \mathbf{S}(\mathbf{t}_k)\mathbf{u} + \mathbf{n}_k, \quad (11)$$

where \mathbf{g}_k is a column vector representing the k -th measurement of all pixels of u , \mathbf{t}_k is a corresponding vector of 2D random displacements, and $\mathbf{S}(\mathbf{t}_k)$ is a matrix, which in every row i has all elements equal to zero except one at the position $i + \mathbf{t}_k(i)$, which is equal to one; see an example of the latent image u and one degraded measurement g in Fig. 1(a) and (b), respectively.

A. Jensen's inequality

We first start with the derivation of discrete equations for Jensen's inequality in (7). Let h denote a discrete version of the prior $p(t)$ and \mathbf{H} denote a matrix performing correlation with h , i.e. $\mathbf{H}\mathbf{u} = \text{vec}(h \star u)$. For example for the displacement prior in (4), h would be a 2D discrete Gaussian function with precision α . Measurements at different positions i 's are independent and thus $p(\mathbf{t}_k) = \prod_i p(\mathbf{t}_k(i))$. It is important to discern that

$$\begin{aligned} \sum_{\mathbf{t}_k} p(\mathbf{t}_k)\mathbf{S}(\mathbf{t}_k)^T &= \mathbf{H}^T, \\ \sum_{\mathbf{t}_k} p(\mathbf{t}_k)\mathbf{S}(\mathbf{t}_k)^T\mathbf{S}(\mathbf{t}_k) &= \mathbf{I}, \\ \sum_{\mathbf{t}_k} \sum_{\mathbf{t}_l} p(\mathbf{t}_k)p(\mathbf{t}_l)\mathbf{S}(\mathbf{t}_k)^T\mathbf{S}(\mathbf{t}_l) &= \mathbf{H}^T\mathbf{H}. \end{aligned} \quad (12)$$

The latent image u is estimated by solving $\frac{d}{du}[-\log p(u|\bar{g})] = 0$, where for $-\log p(u|\bar{g})$ we substitute Jensen's inequality from (7). After some manipulation and using relations in (12), we conclude that the solution is the following linear system:

$$[\mathbf{I} + (K - 1)\mathbf{H}^T\mathbf{H} + \frac{\beta}{\gamma}\mathbf{D}^T\mathbf{D}]\mathbf{u} = K\mathbf{H}^T\bar{\mathbf{g}}. \quad (13)$$

We can see that the above equation is similar to regularized deconvolution of \bar{g} with the blur kernel h (rotated by 180° , since in our formulation \mathbf{H} is a correlation and not convolution matrix). The difference is in the identity matrix \mathbf{I} . As K (the number of measurements in every pixel) grows we approach the classic deconvolution problem. The mean image \bar{g} of many independent measurements reaches $h \star u$ in the limit; see Fig. 2(e). Deconvolution is thus the best possible solution, which Jensen's inequality is consistent with; see Fig. 2(f). As K increases the effect of the regularization term $\mathbf{D}^T\mathbf{D}$ diminishes, which is rational since the noise variance in \bar{g} is inversely proportional to K . However, (13) provides a sub-optimal solution for small K . In the limit case $K = 1$, the solution would be simply $h \star g_1$, if the regularization term was ignored; see Fig. 2(a). If the displacement t is ignored, then h becomes a delta function and (13) simplifies to a regularized least-squares denoising.

B. Variational Bayesian Inference

We can do better for small K using the VB inference. VB alternates between two steps¹: (8) and (9). The first step is similar to Jensen's inequality, but this time we marginalize over estimated $q(\mathbf{t}_k)$, which is in general different for every measurement k and location i , whereas in Jensen's inequality we marginalize over the displacement prior, which is the same everywhere. Let $\mathbf{H}_{q(\mathbf{t}_k)}$ denote a space-variant correlation matrix, which generalizes the original \mathbf{H} by having on every row i the corresponding discrete version of $q(\mathbf{t}_k(i))$. Similar to equalities in (12) we have now

$$\begin{aligned} \sum_{\mathbf{t}_k} q(\mathbf{t}_k)\mathbf{S}(\mathbf{t}_k)^T &= \mathbf{H}_{q(\mathbf{t}_k)}^T, \\ \sum_{\mathbf{t}_k} q(\mathbf{t}_k)\mathbf{S}(\mathbf{t}_k)^T\mathbf{S}(\mathbf{t}_k) &= \text{diag}(\mathbf{H}_{q(\mathbf{t}_k)}^T\mathbf{1}), \\ \sum_{\mathbf{t}_k} \sum_{\mathbf{t}_l} q(\mathbf{t}_k)q(\mathbf{t}_l)\mathbf{S}(\mathbf{t}_k)^T\mathbf{S}(\mathbf{t}_l) &= \mathbf{H}_{q(\mathbf{t}_k)}^T\mathbf{H}_{q(\mathbf{t}_l)}, \end{aligned} \quad (14)$$

where $\mathbf{1}$ denotes a column vector of ones and $\text{diag}(\cdot)$ builds a diagonal matrix from its vector argument. Since $q(u)$ is constrained to delta distributions, we only need to solve $\bar{u} = \arg \min_u -\log q(u)$ in (8), which turns out to be a solution of a linear system

$$\begin{aligned} \left[\frac{1}{K} \sum_k \text{diag}(\mathbf{H}_{q(\mathbf{t}_k)}^T\mathbf{1}) + \frac{1}{K} \sum_k \sum_{l \neq k} \mathbf{H}_{q(\mathbf{t}_k)}^T\mathbf{H}_{q(\mathbf{t}_l)} + \frac{\beta}{\gamma}\mathbf{D}^T\mathbf{D} \right] \bar{\mathbf{u}} \\ = \sum_k \mathbf{H}_{q(\mathbf{t}_k)}^T\bar{\mathbf{g}}. \end{aligned} \quad (15)$$

We apply conjugate gradients to solve this linear system. Since $\mathbf{H}_{q(\mathbf{t}_k)}$ is space-variant, we can not use the Fourier transform to speed up multiplication with this matrix and the inversion is therefore relatively lengthy. A complete knowledge of the discrete distribution $q(t)$ is required to solve this first step. The second step (8) give us means to find $q(t)$. The displacement

¹More precisely, the second step consists of multiple steps and in each we update one factor $q(\mathbf{t}_k)$

t is discrete and bounded and we thus evaluate (8) on a finite set of integer points:

$$q(\mathbf{t}_k(i)) \propto \exp\left(-\frac{\gamma}{2K}(\mathbf{S}(i, \mathbf{t}_k(i))\bar{\mathbf{u}} - \mathbf{g}_k(i))^2 - \frac{\alpha}{2}(\mathbf{t}_k(i))^2\right), \quad (16)$$

where $\mathbf{S}(i, \mathbf{t}_k(i))$ denotes the i -th row of the matrix $\mathbf{S}(\mathbf{t}_k)$. The above equation provides discrete displacement distributions for every pixel and measurement.

The VB inference then iteratively runs (15) and (16). We can notice that $p(t)$ could be a “black box”, since we require only its direct evaluation in (16). For large K , the VB inference converges to Jensen’s inequality in (13), since the first term of the exponent in (16) diminishes and $q(t)$ will resemble more the displacement prior $p(t)$. The superiority of VB over Jensen is apparent for a small number of measurements K as we demonstrate in the next section. In this case VB resembles space-variant blind deconvolution as $q(t)$ is estimated from the data and varies in space.

V. EXPERIMENTS

First, we visually compare the performance of Jensen’s inequality and VB on the following example. Fig. 1(a) shows the original latent image u and Fig. 1(b) shows one measured image g using acquisition model (11) and displacement distribution (4) with the precision $\alpha = 1$. If we estimate the original image from this measurement using Jensen’s inequality in (13), we obtain only a blurred version of the measurement as shown in Fig. 2(a). However, if VB is applied and the empirical displacement distribution is estimated simultaneously, we obtain a perceptually more accurate estimate in Fig. 2(b). We have also compared the denoising output if t is completely ignored and the results were less accurate, which is an indication that the displacement modeling helps the image prior. In the case of two measurements ($K = 2$), both results in Fig. 2(c,d) improve but visually VB still outperforms Jensen. If a large number, e.g. $K = 100$, of independent measurements is available, then the mean observed image \bar{g} in Fig. 2(e) approaches the blurred version of u . Both Jensen and VB converge to the same solution shown in Fig. 2(f) by performing deconvolution of \bar{g} .

In addition to the visual comparison, we compare performance using two well-known objective quality metrics, the peak-signal-to-noise ratio (PSNR) and the structural similarity index measure (SSIM) [8]. We summarize the performance for two sets of parameters. Fig. 3 shows results for moderate weights $\gamma = 10$ and $\beta = 1$. Fig. 4 shows results for $\gamma = 10^4$ and $\beta = 10^3$, which corresponds to a more aggressive behavior of the VB inference, i.e., relying more on data and less on the displacement prior $p(t)$. The parameters were chosen such that the ratio β/γ in both sets was constant to keep the same effect of image regularization in (13) and (15). Each graph plots PSNR or SSIM versus the number of measurements K for three methods: mean image \bar{g} (dotted line), Jensen’s inequality (13) (dashed line), and VB (15)-(16) (solid line). The mean-image performance is a baseline and both Jensen and VB perform better by a large margin. For moderate parameters (Fig. 3), VB outperforms Jensen both in terms of PSNR and

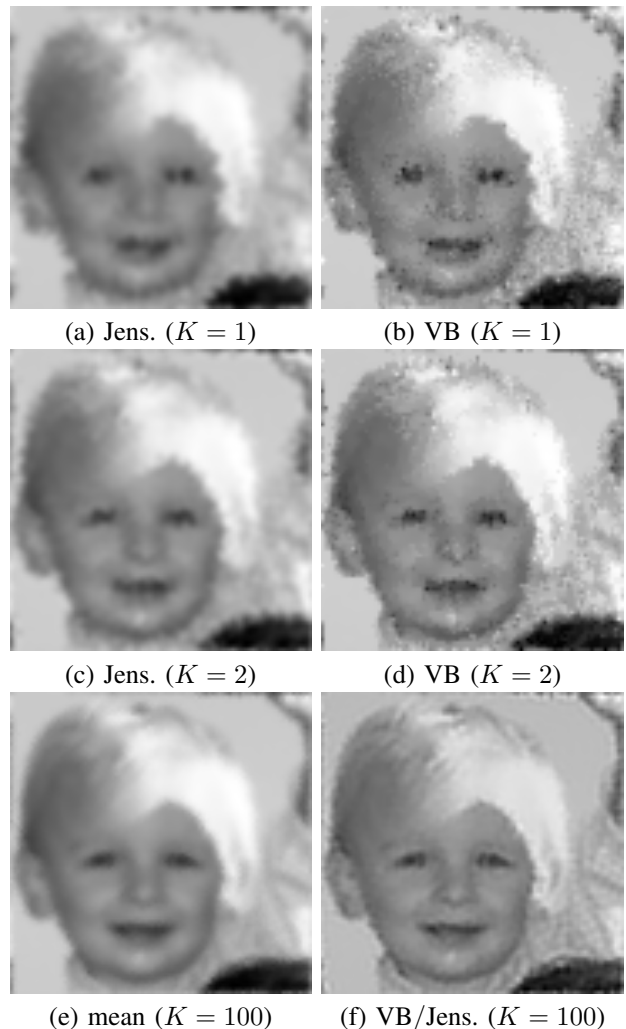
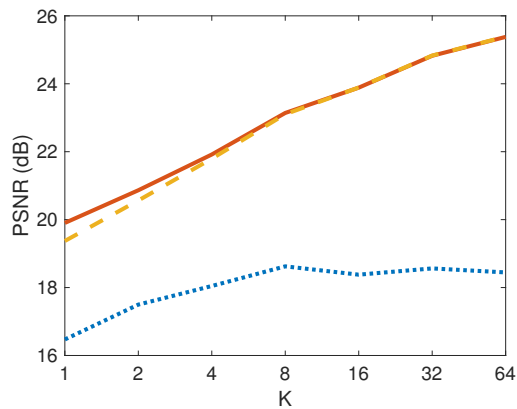


Fig. 2. 2D image reconstruction results: (a) inference with Jensen’s inequality from a single measurement, (b) Variational Bayesian inference from a single measurement, (c) inference with Jensen’s inequality from two measurements, (d) Variational Bayesian inference from two measurements, (e) mean image of 100 measurements, (f) inference from 100 measurements with Variational Bayes (or Jensen’s inequality, which provides almost identical results).

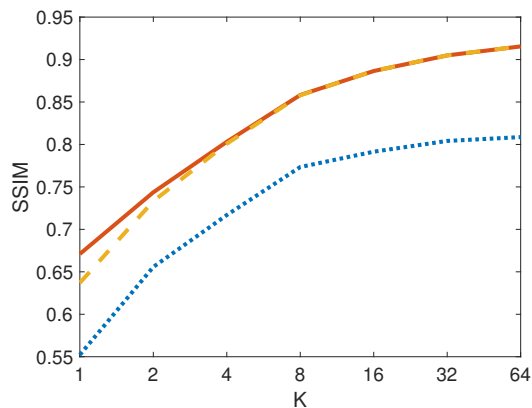
SSIM for small $K \leq 4$, and the VB gain vanishes for large K as predicted. In the case of the aggressive parameter setting (Fig. 4), the advantage of VB is even more apparent but only in terms of SSIM. PSNR is biased towards over-smoothed results and therefore it favors images obtained with Jensen’s inequality, which are overly blurred; compare $K = 2$ Jensen’s result in Fig. 1(c) with the VB result in Fig. 1(d). In terms of PSNR both images are almost identical but we can see that the VB result is sharper, which is reflected by better SSIM in Fig. 4(b).

VI. CONCLUSION

We have introduced an acquisition model with localization uncertainty that we believe describes a measurement phenomenon present in many different scientific fields. We have derived a general Bayesian solution to the model through marginalization over nuisance variables using either Jensen’s



(a) PSNR



(b) SSIM

Fig. 3. Performance evaluation for parameters $\gamma = 10$ and $\beta = 1$: (a) PSNR versus number of measurements K , (b) SSIM versus number of measurements K . Curves represent performance of the mean image \bar{g} (blue dotted), Jensen's inequality (yellow dashed), and Variational Bayesian inference (red solid).

inequality or Variational Bayesian inference. Final discrete equations were presented for the 2D image reconstruction case and the relation with deconvolution was hinted.

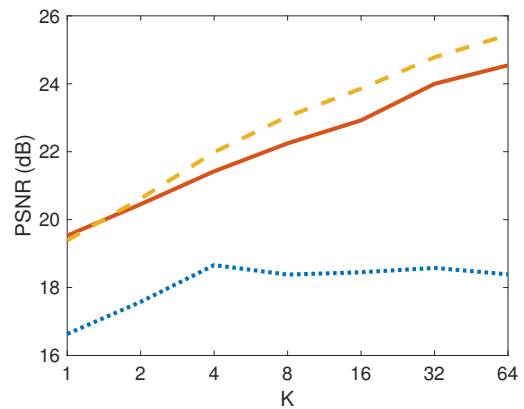
We plan to validate the model and its Bayesian solution on 3D volume reconstruction in free-hand 2D ultrasound imagery. A possible extension of the model is to incorporate interpolation in the sampling operator to allow for continuous values of displacement. We also seek to explore the possibility to use this approach for image blind deconvolution.

ACKNOWLEDGMENT

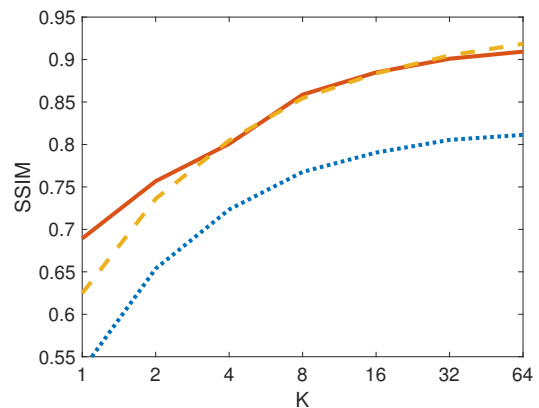
The authors would like to acknowledge support provided by GACR grant GA13-29225S and partially by TACR grant TA04011392.

REFERENCES

- [1] E. Betzig, G. H. Patterson, R. Sougrat, O. W. Lindwasser, S. Olenych, J. S. Bonifacino, M. W. Davidson, J. Lippincott-Schwartz, and H. F. Hess, "Imaging intracellular fluorescent proteins at nanometer resolution," *Science*, vol. 313, no. 5793, pp. 1642–1645, 2006.
- [2] A. Gee, R. Prager, G. Treece, and L. Berman, "Engineering a freehand 3d ultrasound system," *Pattern Recognition Letters*, vol. 24, no. 45, pp. 757–777, 2003.



(a) PSNR



(b) SSIM

Fig. 4. Performance evaluation for parameters $\gamma = 10^4$ and $\beta = 10^3$: (a) PSNR versus number of measurements K , (b) SSIM versus number of measurements K . Curves represent performance of the mean image \bar{g} (blue dotted), Jensen's inequality (yellow dashed), and Variational Bayesian inference (red solid).

- [3] D. Laksameethanathan and S. Brandt, "A Bayesian reconstruction method with marginalized uncertainty model for camera motion in microrotation imaging," *IEEE Transactions on Biomedical Engineering*, vol. 57, no. 7, pp. 1719–1728, 2010.
- [4] R. Sundareswara and P. R. Schrater, "Bayesian discounting of camera parameter uncertainty for optimal 3d reconstruction from images," *Computer Vision and Image Understanding*, vol. 115, no. 1, pp. 117–126, 2011.
- [5] Y. Chi, L. L. Scharf, A. Pezeshki, and A. R. Calderbank, "Sensitivity to basis mismatch in compressed sensing," *IEEE Transactions on Signal Processing*, vol. 59, no. 5, pp. 2182–2195, May 2011.
- [6] S. D. Babacan, R. Molina, M. N. Do, and A. K. Katsaggelos, "Bayesian blind deconvolution with general sparse image priors," in *ECCV*, ser. Lecture Notes in Computer Science, A. W. Fitzgibbon, S. Lazebnik, P. Perona, Y. Sato, and C. Schmid, Eds., vol. 7577. Springer, 2012, pp. 341–355.
- [7] R. Molina, J. Mateos, and A. K. Katsaggelos, "Blind deconvolution using a variational approach to parameter, image, and blur estimation," *IEEE Transactions on Image Processing*, vol. 15, no. 12, pp. 3715–3727, Dec. 2006.
- [8] Z. Wang, A. Bovik, H. Sheikh, and E. Simoncelli, "Image quality assessment: from error visibility to structural similarity," *IEEE Transactions on Image Processing*, vol. 13, no. 4, pp. 600–612, 2004.